Correlation between temperature variations of static and dynamic properties in glass-forming liquids

D. N. Voylov, P. J. Griffin, B. Mercado, J. K. Keum, M. Nakanishi, V. N. Novikov, and A. P. Sokolov

Phys. Rev. E **94**, 060603 — Published 29 December 2016

DOI: 10.1103/PhysRevE.94.060603

Correlation between temperature variations of static and dynamic properties in glass forming liquids

D.N Voylov[1], P.J. Griffin[2], B. Mercado[3], J.K. Keum[4], M. Nakanishi[5], V.N. Novikov[1], A.P. Sokolov[1,6]

[1]*Department of Chemistry, University of Tennessee, Knoxville, TN 37996, USA*

[2]*Department of Materials Science and Engineering, University of Pennsylvania, Philadelphia, PA 19104-6272, USA*

[3]*Chemistry Department, Yale University, New Haven, CT 06511, USA*

[4]*Spallation Neutron Source, Oak Ridge National Laboratory, Oak Ridge, TN 37831, USA*

[5]*Department of Electrical Engineering, Fukuoka Institute of Technology, Fukuoka 811-0295, Japan*

[6]*Chemical Sciences Division, Oak Ridge National Laboratory, Oak Ridge, TN 37831, USA*

Abstract

Detailed analysis of the static structure factor *S(Q)* in several glass forming liquids reveals that the temperature variations of the width of the main diffraction peak $\Delta Q(T)$ correlates with fragility of these liquids. This observation suggests a direct connection between rather subtle structural changes and sharp slowing down of structural relaxation in glass forming liquids. We show that this observation can be rationalized using the Adam-Gibbs approach, through a connection between temperature variations of structural correlation length, $l_c \sim 2\pi/\Delta Q$, and the size of cooperatively rearranging regions.

Despite decades of intensive studies, the microscopic mechanism of the sharp slowing down in dynamics of liquids upon cooling, i.e. of the glass transition, remains a puzzle [1-4]. The structural relaxation time $\tau_\alpha(T)$ and viscosity $\eta(T)$ in many glass-forming liquids increase by 10-12 orders when temperature is changed by ~15-20% close to their glass transition temperature T_g [1,2]. Yet structure of these liquids shows no significant changes. To characterize the steepness of the temperature dependence of $\tau_\alpha(T)$ and $\eta(T)$, the fragility index *m* has been introduced [1,5]:

$$m = \left. \frac{d \log_{10} \tau_\alpha}{d(T_g / T)} \right|_{T=T_g} \qquad (1)$$

A steeper variation of τ_α with T_g/T (at T_g) corresponds to a higher fragility index. It has been recognized that fragility depends strongly on the type of interatomic/intermolecular bonds and is relatively low (*m*~20-35) in covalent bonded systems, intermediate (*m*~40-60) in many hydrogen bonded systems, and high (*m*~60-100) in Van der Waals and ionic liquids [6]. Liquids with low fragility index are termed *strong*, while those with high fragility index are termed *fragile*.

These empirical connections between liquid fragility and the types of local interactions have inspired several attempts to relate liquid structure to fragility [7-12]. For example, the authors of [7,8] attempted to connect fragility to the number of edge-sharing tetrahedral units in covalent bonded systems. Significant efforts were devoted to analysis of changes in static structure factor S(Q) in various liquids during glass transition [9-11]. A correlation between the so-called van der Waals peak position in S(Q) and fragility was found for poly(n-alkyl methacrylates) [12]. Intensive studies have been performed on bulk metallic glass-formers [13-17]. Zhao et al [13] analyzed temperature variations in the width $\Delta Q(T)$ of the main diffraction peak in several Au-Si, Cu-Ag and In-Sn liquids, and introduced the structural fragility parameter,

$F_s = d[l/l(T^*)]/d(T^*/T)|_{T=T^*}$. Here $l \approx 2\pi/\Delta Q$ is the correlation length of disordered structure, and T* is the temperature ~10K above the liquidus temperature of these liquids. The authors demonstrated that the so-defined structural fragility correlates with glass-forming ability of the systems: smaller F_s corresponds to higher glass-forming ability [13]. Although the authors did not compare these data to the dynamic fragility index *m*, their results imply that there might be a correlation between F_s and *m*. It should be noted that other studies have revealed significant temperature changes in ΔQ(T) in both the strong glass-former B_2O_3 [10] and the fragile glass-former $Ca_{0.4}K_{0.6}(NO_3)_{1.4}$ (CKN) [11], leading the authors of [9] to conclude that there is no correlation between changes in the diffraction peak width and fragility. This comparison may not be valid, however, because the local coordination of the boron atom in borate glasses changes close to T_g [18,19], strongly affecting both S(Q) and ΔQ(T).

Another definition of structural fragility γ has been introduced recently in [14-17]. γ is defined as the mismatch between the amplitude of the static structure peak $S(Q_{max})_{meas}$ measured at T_g and the linear extrapolation of the temperature dependence of $S(Q_{max},T)$ to T_g from high temperatures $T>>T_g$: $\gamma = [S(Q_{max})_{meas} - S(Q_{max},T_g)_{extrapol}]/S(Q_{max})_{meas}$. The authors found correlation between γ and a similar kinetic fragility parameter *D**, which is estimated from fits of viscosity using the Vogel-Fulcher-Tammann (VFT) function, $\eta = \eta_0 exp\left(\frac{D^*T_0}{T-T_0}\right)$ at high temperatures $T > 1.8T_g$. The nature of this correlation has not been explained and remains unknown.

To verify a possible relationship between temperature variations in the static structure factor and fragility *m*, we performed detailed studies of S(Q) in several glass forming materials. Our analysis revealed clear correlations between fragility *m* and the temperature variation of the width of the main diffraction peak ΔQ(T) in S(Q), suggesting a connection between changes in

the characteristic structural correlation length and the steepness of temperature variations of $\tau_\alpha(T)$ in glass-forming liquids. Moreover, these observations provide an explanation for the reported correlation (Refs. [14-17]) between changes in the amplitude of $S(Q_{max})$ and fragility. Based on these observation we suggest that the subtle changes in the static correlation length of liquids may be at the origin of the steep temperature variations of $\tau_\alpha(T)$ and $\eta(T)$.

We focus our study on several model glass-formers: glycerol (m=53, T_g = 190K [20]), sucrose benzoate (SB) (m=94, T_g = 337K [20]), propylene carbonate (PC) (m=93, T_g = 157K [20]), all purchased from Sigma-Aldrich; and low molecular weight (M_w=500 g/mol) polystyrene (PS0.5k) (m=72, T_g =253K [21]), purchased from Polymer Source, Inc. The X-ray diffraction of PS, PC and glycerol was measured using a Rigaku MicroMax-007HF source (Cu Kα; λ = 1.54178 Å) coupled to a Saturn994+ CCD detector. A meniscus of the material in a liquid state was suspended in a 0.2mm loop of a MiTeGen magnetic pin (MiTeGen, LLC, Ithaca, NY, USA), and then transferred onto an AFC11 goniometer. Line profiles of the 2D diffraction data were integrated and processed with the Rigaku 2DP software package. The contribution of the X-ray scattering from magnetic pin and air was measured separately at each of the measured temperatures and subtracted as the background correction from the X-ray scattering signal of the sample. The X-ray scattering of sucrose benzoate was measured using a PANalytical X'Pert Pro MPD equipped with an X'Celerator solid-state detector and XRK-900 heating chamber. For the XRD measurements, X-rays were generated at 45 kV/40 mA, and the X-ray wavelength was λ=1.5406 Å (Cu Kα radiation).

In our analysis, we focused on the width $\Delta Q(T)$ of the main diffraction peak in the measured S(Q) (Fig.1). To broaden the number of glass-forming systems in this analysis, we also used available in literature high accuracy diffraction data for $GeSe_2$ [22] (T_g = 663K), Na_2O-

$2B_2O_3$ [23] (T_g = 748K), K_2O-$2SiO_2$ [23] (T_g = 768K), K_2O-$3SiO_2$ [23] (T_g = 760K), o-terphenyl (OTP) [24] (T_g = 246K), propylene glycol (PG) [25] (T_g = 160K), phenyl salicylate (salol) [26] (T_g = 220K), PC [26] (T_g = 158K) and room-temperature ionic liquids N1444.NTf2 [27] (T_g = 205K) and bmim.PF_6 [28] (T_g = 194K). We fit the S(Q) using mainly one or two Lorentzian functions (to take into account a small pre-peak at lower Q in some of the materials) in the Q-range only slightly above the Q_{max} (some examples are in Fig. 1). We specifically excluded the high-Q tail of the main peak from the fit because in some systems it is affected by contributions of higher-Q diffraction peaks (see, e.g., PC in Fig.1). Excluding the right wing of the peak was not essential for the fit, which was robust because of the very high accuracy of the measurements. The fit by three Lorentzian functions has been used only for data of salol and N1444.NTf2 systems, where diffraction peaks strongly overlap. However, these peaks are sufficiently structured to make the fit by three Lorentzian functions quite robust. As an example, the fit of salol at T=190K is shown in Fig. 1. The results of all the fits, including the error-bars and the Q-interval used in the fits are presented in the Table 1. Our analysis reveals that $\Delta Q(T)$ (defined as FWHM) indeed shows a measurable decrease upon cooling at $T > T_g$. Moreover, the temperature dependence of $\Delta Q(T)$ varies significantly between different materials (Fig. 2).

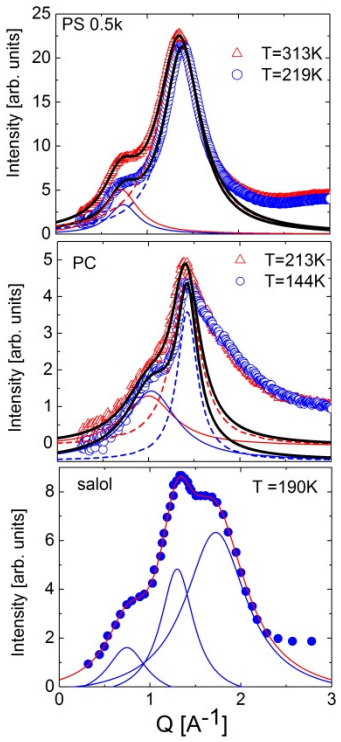

FIG.1 X-ray scattering data for polystyrene (PS) MW=500 g/mol, propylene carbonate (PC) and salol. Symbols present experimental data. For PS and PC the data in a glassy state at T~0.9 T_g (blue circles) and in a liquid state at T~1.3T_g (red triangles). Thick solid lines correspond to the fit by a sum of two Lorentzian functions, which are shown by dashed and thin solid lines. Only the data in a glassy state and their fit by three Lorentzian functions are shown for salol.

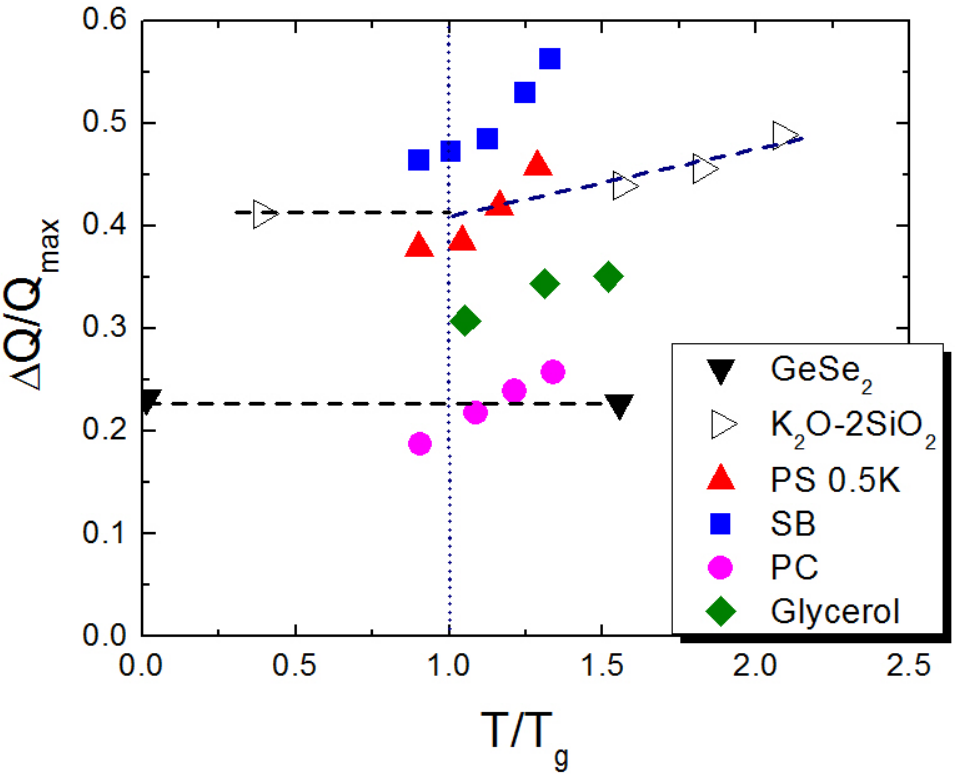

FIG. 2. Dependence of the diffraction peak width normalized by the peak position $\Delta Q/Q_{max}$ vs T/T_g for materials with wide variations in fragility (from $GeSe_2$ with m=32 to PC with m=100). The error bars are within the symbol size.

Detailed analysis of the data reveals that strong glass-former $GeSe_2$ shows the same $\Delta Q/Q_{max}$ at T=10K and T=1084K, which are far below and far above T_g. At the same time, $\Delta Q(T)$ changes significantly at temperatures above T_g for very fragile SB, while it changes less for less fragile glycerol (Fig. 2). To compare temperature variations of $\Delta Q(T)$ in different systems, we used two approaches. In both approaches we analyzed change in the width of the main diffraction peak between glass and liquid states (the obtained fit parameters for the analyzed liquids and error-bars are presented in the Table 1). In glass state we take $\Delta Q_{glass} = \Delta Q(T\sim0.9T_g)$. We note that below T_g ΔQ has very weak variations, and the measured at $T\sim0.9T_g$ width essentially

corresponds to the equilibrium width of the peak at T_g. In a liquid state, ΔQ_{liq} was chosen in two different ways. In the first approach we use ΔQ_{liq} at some temperature which has the fixed ratio to T_g for all the materials, namely $\Delta Q_{liq} = \Delta Q(T_{liq} \sim 1.3T_g)$. The liquid temperature T_{liq} was chosen arbitrarily to be above T_g, but not very high, where the most data for different systems exists. In the second approach, ΔQ_{liq} was taken at a temperature where the structural relaxation time is in the range $\tau_\alpha \sim 10^{-7}$-10^{-9} s. This interval is chosen arbitrarily in the middle of the interval of $\log\tau_\alpha$ between T_g and the high temperature limit of the relaxation time. Specifically, the following τ_α were used: bmim.PF6: $\sim 10^{-7}$ s, salol: ~ 3 10^{-9} s, OTP, N1444.Ntf2, PC, SB, PS0.5K: $\sim 10^{-8}$ s. In $GeSe_2$, K_2O-$2SiO_2$, and K_2O-$3SiO_2$ the width changes very weakly with T, so $\delta\Delta Q_{liq}/\Delta Q_{glass}$ is very small at all T anyway. In $GeSe_2$ we assume $\delta\Delta Q_{liq} = 0$, in K_2O-$2SiO_2$, and K_2O-$3SiO_2$ ΔQ_{liq} was taken at T = 1200K at which viscosity η of these melts is about 10^3 Poise [1]. This value of viscosity is by a factor 10^{-10} lower than viscosity at T_g, $\eta(T_g) = 10^{13}$ Poise, and thus roughly corresponds to $\tau_\alpha \sim 10^{-8}$ sec (assuming $\tau_\alpha(T_g) = 10^2$ sec).

The relative change of the peak width can be estimated as:

$$\frac{\delta\Delta Q}{\Delta Q_{glass}} = \frac{\Delta Q_{liq} - \Delta Q_{glass}}{\Delta Q_{glass}} \qquad (2)$$

It appears that the so-defined relative change in the width of the main diffraction peak for both approaches correlates with the fragility of analyzed here glass forming liquids (Fig. 3a,b). The $\delta\Delta Q/\Delta Q_{glass}$ changes by more than 30% in the most fragile liquid PC, by ~10% for intermediate fragility liquids such as glycerol and PG, while there is almost no change for materials with fragility below 32 (Fig.3). We emphasize that the obtained results for the change in the width of the main diffraction peak, $\delta\Delta Q$, are independent of the number of Lorentzians chosen for the fit (see Table 1).

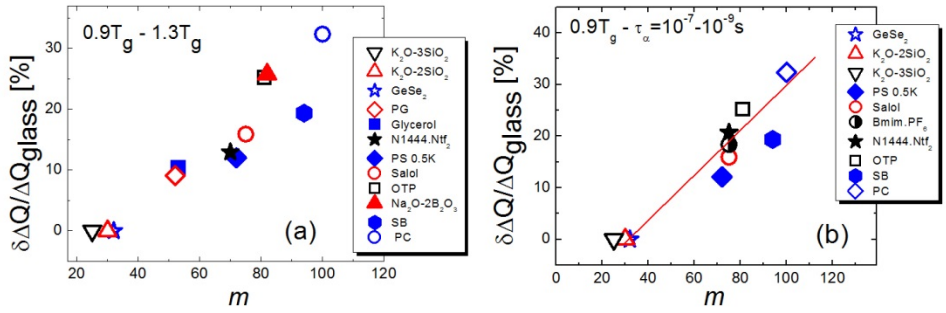

FIG. 3. The relative change in the width of the main diffraction peak (Eq. (2)) vs fragility for several glass forming systems. (a) ΔQ_{liq} was chosen at T = 1.3T$_g$; (b) ΔQ_{liq} was chosen at temperature when $\tau_\alpha \sim 10^{-7}$-10^{-9} s. The error bars are within the symbol size.

These results clearly demonstrate that there might be a relationship between temperature variations in the static structure and the steepness of the temperature variations of structural relaxation (fragility). These observations also provide an explanation for the discovered (Refs. [14-17]) correlation of the amplitude mismatch of the diffraction peaks γ and fragility. In the case of strong systems, where ΔQ does not change with temperature (Fig. 3), the change of the peak amplitude is essentially controlled by the Debye-Waller factor. So, the extrapolation of the peak amplitude from high T to T$_g$ should show no significant mismatch, i.e. low γ. In contrast, significant narrowing of the diffraction peak with decreasing temperature above T$_g$ in fragile systems will lead to an additional increase of its amplitude, exceeding simple linear extrapolation. As a result, the mismatch between the high-T extrapolated amplitude and the data measured at T$_g$ is expected in fragile systems due to change of ΔQ not accounted for in this extrapolation. Systems with higher fragility exhibit larger changes in the peak width (Fig. 3) and should therefore exhibit larger mismatch γ.

While the microscopic origin of the width ΔQ of the main diffraction peak can be different in different types of molecular glasses, the width ΔQ in most cases can be related to a characteristic correlation length of the disordered structure, $l_c \sim 2\pi/\Delta Q$. This length scale l_c is traditionally associated with medium range order [30-32], although the respective structural units might be of different nature, e.g. repeating basic structural units determined by the short-range order [33], nano-voids [34], or rings [35]. However, additional broadening of the diffraction peak can be also due to a distribution of the distances between the structure units or sizes of voids. Nevertheless, let us assume that the main contribution to the peak broadening is due to changes in the structural correlation length l_c. In that case, more fragile systems have larger variations in l_c, while stronger liquids have essentially the same l_c in liquid and glassy states. The variation in l_c might be interpreted as a change in structural disorder with temperature in the case of fragile liquids, while the degree of static disorder apparently remains about the same in a liquid and glassy state in strong systems.

We are not aware of any theoretical predictions connecting changes in the static structure to fragility. However, the observed evolution of l_c with temperature can be compared with changes of the activation energy of structural relaxation in the Adam-Gibbs theory [36]. According to the theory [36], the structural relaxation events are cooperative and occur in cooperatively rearranging regions (CRR). Adam-Gibbs theory assumes that the activation energy E of the structural relaxation is proportional to the number of particles in a CRR and to its volume $E \propto L^3$, where L is a characteristic CRR size. Thus, according to the theory, higher fragility should be related to the larger increase in L [36]. This was recently confirmed by non-linear dielectric spectroscopy measurements in a few molecular glass-formers [37,38]. Non-linear dielectric spectroscopy provides estimates of the number of cooperatively rearranging

units $N_{coop}(T)$, and detailed analysis indeed revealed that $N_{coop}(T)$ varies much stronger in fragile liquids than in strong ones [37]. Following the Adam-Gibbs approach, we can write:

$$L(T) \propto \sqrt[3]{E(T)} = \sqrt[3]{kTln\frac{\tau_\alpha(T)}{\tau_0}} \quad (3)$$

We can compare temperature variations of the so-defined size of CRR between T_g and $1.3T_g$ to the observed changes in the diffraction peak width in the same temperature range (Fig. 3). The latter can be expressed through the correlation length l_c. This comparison (Fig. 4a) indeed reveals a positive correlation between relative changes in L and in l_c for the systems with sufficient data to analyze. Note, that τ_α data for some of the materials presented in the Fig. 3 are not available in the required temperature range, so they are not shown in Fig. 4a. Surprisingly, we find a one-to-one, quantitative connection between $L(1.3T_g)/L(T_g)$ and $l_c(1.3T_g)/l_c(T_g)$ (Fig. 4a), strongly emphasizing that there might be a direct relationship between rather subtle (~10%-30%) changes in the static structure of liquids and the temperature dependence of their structural relaxation (and viscosity). For consistency, we also checked the relation between the temperature dependence of log τ_α(T) and that of $l_c(T)^3$ (Eq.3). In Fig. 4b log τ_α(T) is plotted as a function of $l_c(T)^3/T$ normalized to its value at T_g for the measured here PS, SB, PC and glycerol. The universal linear dependence is observed for all four materials regardless of their fragility without any adjustable parameters. These observations suggest a connection of the growing length scale of CRR in supercooled liquids with their growing structural correlation length extracted from the main diffraction peak. This finding is in agreement with Refs. [3,39] where, using MD simulations, it was shown that the influence of the boundary propagates into the bulk supercooled liquid over increasing length scales on cooling, suggesting that the static correlation length increases with cooling. In the case of covalent bonded systems, these structures are well defined already in the liquid state and are nominally temperature independent above T_g. As a

result, the activation energy controlling the rate of structural relaxation is also essentially temperature independent, and $\tau_\alpha(T)$ exhibits nearly Arrhenius temperature dependence. In contrast, Van der Waals and ionic liquids don't have well defined locally favored structures. As a result, correlations in their static structure grow more readily upon cooling. Correspondingly, the activation energy controlling structural relaxation increases strongly on cooling, leading to high steepness of the temperature dependence of $\tau_\alpha(T)$ and $\eta(T)$ (high fragility).

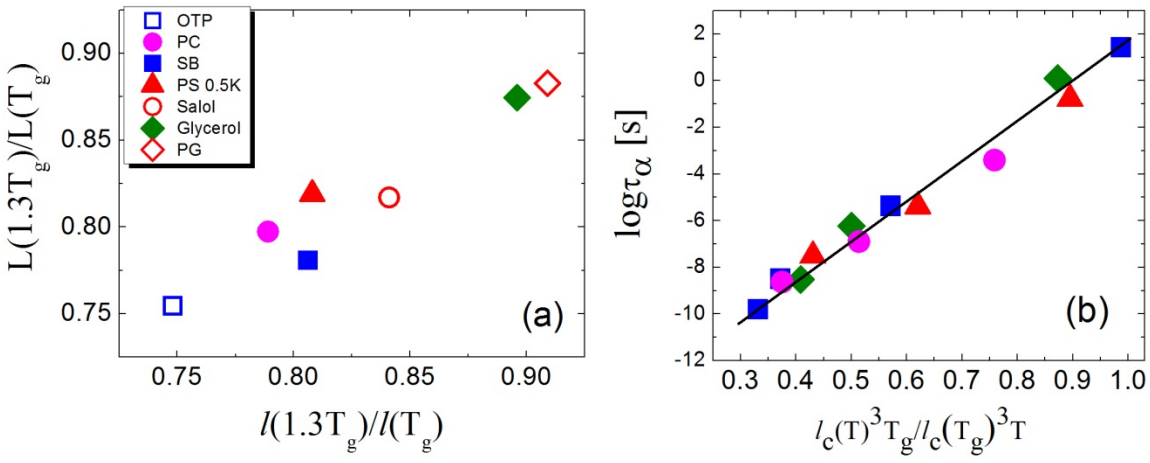

FIG. 4 a) Correlation between the ratio of the CRR sizes $L(1.3T_g)/L(T_g)$ and the ratio of the structural correlation lengths $l_c(1.3T_g)/l_c(T_g)$. Materials shown and reference for $\tau_\alpha(T)$ are the following: orthotherphenyl (OTP) [40], propylene carbonate (PC) [41], sucrose benzoate (SB) [42], polystyrene (PS) oligomer with MW = 0.5 kg/mol [43], salol [44], glycerol [41], propylene glycol (PG) [41]; b) The dependence of log $\tau_\alpha(T)$ on $l_c(T)^3/T$ normalized to its value at T_g for PS, SB, PC and glycerol. Symbols are the same as in Fig. 4a.

In conclusion, our analysis reveals that temperature variations in the width of the main diffraction peak differ significantly between different glass forming liquids. These changes are negligible in low fragility (strong) materials, while they are significant in high fragility liquids. The observed correlation between relative changes in ΔQ(T) and fragility suggests a strong connection between temperature variations in static structural correlations and the dynamics of glass forming liquids. Furthermore, this temperature evolution of the structural correlation length is consistent with the changes in the CRR size estimated following Adams-Gibbs theory. The observed ~30% changes in the structural correlation length l_c of fragile liquids leads to sharp slowing down of structural relaxation time. This might be explained by the exponential dependence of τ_α(T) on l_c, $\log \tau_\alpha/\tau_0 \propto L^a \propto l_c^a$, with $a \sim 3$. We want to emphasize that the observed correlations may not work for all glass forming systems. We specifically exclude polymers from this analysis, because they usually show deviations from many correlations known for non-polymeric systems [45-47]. We also excluded B_2O_3, because of its structural changes in the same temperature range [18,19]. Nevertheless, the observed correlation between subtle temperature changes in S(Q) and fragility provides insight into the microscopic mechanism controlling the dynamics of glass forming liquids.

Acknowledgments: UTK team acknowledges support from the NSF Polymer program (grant DMR-1408811).

References

[1] C. A. Angell, Science **267**, 1924 (1995).

[2] P. G. Debenedetti and F. H. Stillinger, Nature **410**, 259 (2001).

[3] L. Berthier and G. Biroli, Rev. Mod. Phys. **83**, 587 (2011).

[4] P. W. Anderson, Science **267**, 1615 (1995).

[5] C. A. Angell, J. Non-Cryst. Solids **73**, 1 (1985).

[6] R. Böhmer, K.L. Ngai, A.C. Angell, D. J. Plazek, J. Chem. Phys. **99**, 4201 (1993).

[7] M. Wilson and P. S. Salmon, Phys. Rev. Lett. **103**, 157801 (2009).

[8] A. Zeidler, P. S. Salmon, R. A. Martin, T. Usuki, P. E. Mason, G. J. Cuello, S. Kohara, and H. E. Fischer, Phys. Rev. B **82**, 104208 (2010).

[9] N. Zotov, R. G. Delaplane, and H. Keppler, Phys. Chem. Miner. **26**, 107 (1998).

[10] D. Engberg, J. Swenson, A. Wannberg, L. Börjesson, NFL Experimental Report: SLAD14 - SLAD15 (1996).

[11] C. Tengroth, J. Swenson, L. Börjesson, Physica B **234 & 236**, 414 (1997).

[12] G. Floudas and P. Stepanek, Macromolecules **31**, 6951 (1998).

[13] Y. Zhao, X. Bian, X. Qin, J. Qin, and X. Hou, Phys. Lett. A **367**, 364 (2007).

[14] N. A. Mauro, M. Blodgett, M. L. Johnson, A. J. Vogt, and K. F. Kelton, Nature Commun. **5**, 1 (2014).

[15] N.A. Mauro, A. J. Vogt, M. L. Johnson, J. C. Bendert, R. Soklaski, L. Yang, K.F. Kelton, Acta Mater. **61**, 7411 (2013).

[16] N. A. Mauro, A. J. Vogt, M. L. Johnson, J. C. Bendert, and K. F. Kelton, Appl. Phys. Lett. **103**, 021904 (2013).

[17] N.A. Mauro, M.L. Johnson, J.C. Bendert, K.F. Kelton, J. Non-Cryst. Sol. **362**, 237 (2013).

[18] A. C. Wright, G. Dalba, F. Rocca, N.M. Vedishcheva, Phys. Chem. Glasses: Eur. J. Glass Sci. Technol. B **51**, 233 (2010).

[19] M. Misawa, J. Non-Cryst. Sol. **122**, 33 (1990).

[20] Q. Qin, G.B. McKenna, J. Non-Cryst. Sol. **352**, 2977 (2006).

[21] P. G. Santangelo, C.M. Roland, Macromolecules **31**, 4581 (1998).

[22] S. Susman, K. J. Volin, D. G. Montague, and D. L. Price, J. Non. Cryst. Solids **125**, 168 (1990).

[23] F. Kargl, *The Interplay of Structure and Microscopic Dynamics in Oxidic Melts Observed by Means of Inelastic Neutron Scattering*, (Technischen Universitat Munchen Lehrstuhl fur Experimentalphysik 4, 2006).

[24] A. Tölle, Reports Prog. Phys. **64**, 1473 (2001).

[25] R. L. Leheny, N. Menon, S. R. Nagel, D. Long Price, K. Suzuya, and P. Thiyagarajan, J. Chem. Phys. **105**, 7783 (1996).

[26] E. Eckstein, J. Qian, R. Hentschke, T. Thurn-Albrecht, W. Steffen, and E. W. Fischer, J. Chem. Phys. **113**, 4751 (2000).

[27] C. S. Santos, H. V. R. Annapureddy, N. S. Murthy, H. K. Kashyap, E. W. Castner, and C. J. Margulis, J. Chem. Phys. **134**, 064501 (2011).

[28] A. Triolo, A. Mandanici, O. Russina et al, J. Phys. Chem. B **110**, 21357 (2006).

[29] J. O'M. Bockris, J. D. Mackenzie and J. A. Kitchener, Trans. Faraday Soc. **51**, 1734 (1955).

[30] P.H. Gaskell, D.J. Wallis, Phys. Rev. Lett. **76**, 66 (1996).

[31] P.S. Salmon, R.A. Martin, P.E. Mason, and G.J. Cuello, Nature (London) **435**, 75 (2005).

[32] A.P. Sokolov, A. Kisliuk, M. Soltwich and D. Quitmann, Phys. Rev. Lett. **69**, 1540 (1992).

[33] N. Als-Nielsen and D. McMorrow, *Elements of Modern X-ray Physics* (John Wiley & Sons, New York, 2011).

[34] S. R. Elliott, Phys. Rev. Lett. **67**, 1477 (1991).

[35] S. Susman, D. L. Price, K. J. Volin, R. J. Dejus, and D. G. Montague, J. Non. Cryst. Sol. **106**, 26 (1988).

[36] G. Adam and J. H. Gibbs, J. Chem. Phys. **43**, 139 (1965).

[37] Th. Bauer, P. Lunkenheimer, and A. Loidl, Phys. Rev. Lett. 111, 225702 (2013).

[38] S. Albert, Th. Bauer, M. Michl, G. Biroli, J.-P. Bouchaud, A. Loidl, P. Lunkenheimer, R. Tourbot, C. Wiertel-Gasquet, F. Ladieu, Science **352**, 1308 (2016).

[39] G. Biroli, J.-P. Bouchaud, A. Cavagna, T. S. Grigera and P. Verrocchio, Nature Phys. **4**, 771 (2008).

[40] N. Petzold, B. Schmidtke, R. Kahlau, D. Bock, R. Meier, B. Micko, D. Kruk, and E.A. Rössler, J. Chem. Phys. **138**, 12A510 (2013).

[41] P. Lunkenheimer, R. Wehn, U. Schneider, and A. Loidl, Phys. Rev. Lett. **95**, 055702 (2005).

[42] J.R. Rajian and E.L. Quitevis, J. Chem. Phys. **126**, 224506 (2007).

[43] C.M. Roland, R. Casalini, J. Chem. Phys. **119**, 1838 (2003).

[44] F. Stickel, E.W. Fischer, and R. Richert, J. Phys. Chem. **102**, 6251 (1995).

[45] T. Scopigno, D. Cangialosi, and G. Ruocco, Phys. Rev. B **81**, 100202(R) (2010).

[46] V. N. Novikov, Y. Ding, and A. P. Sokolov, Phys. Rev. E **71**, 061501 (2005).

[47] J. Colmenero, J. Phys.: Condens. Matter **27**, 103101 (2015).

Table 1. Fitting results for all analyzed data. N is the number of Lorentzians in the fitting function. In cases when there are a few versions of the fit (different N), we use the one with the largest N (e.g., in Fig.3 the version with N=3 for salol is shown).

Material	$\Delta Q_{0.9Tg}$, A^{-1}	$\Delta Q_{1.3Tg}$, A^{-1}	$Q_{0.9Tg}$, A^{-1}	$Q_{1.3Tg}$, A^{-1}	$\delta\Delta Q$, %	N	Q range, $Å^{-1}$
Salol	0.6±0.015	0.69±0.016	1.31±0.021	1.29±0.025	15	1	1.03-1.38
	0.51±0.03	0.59±0.01	1.31±0.015	1.28±0.011	15.7	2	0.6-1.38
	0.44±0.005	0.51±0.003	1.3±0.002	1.27±0.002	15.9	3	0.3-1.38
Na_2O-$2B_2O_3$	0.4±0.0042	0.5±0.0062	1.38±0.0013	1.35±0.0014	25.8	1	0.6-1.44
OTP	0.41±0.03	0.52±0.02	1.46±0.003	1.43±0.005	25	1	1.2-1.48
N1444Ntf2	0.48±0.005	0.55±0.007	1.46±0.001	1.41±0.001	14.6	1	0.5 -1.68
	0.425±0.006	0.48±0.003	1.46±0.001	$1.41±6\ 10^{-4}$	13	2	0.5-1.68
K_2O-$2SiO_2$	0.39±0.02	0.39±0.012	0.96±0.005	0.89±0.003	0	1	0.32-1
K_2O-$3SiO_2$	0.48±0.02	0.48±0.025	0.865±0.006	0.81±0.006	0	1	0.2-0.9
$GeSe_2$	0.23±0.01	0.23±0.01	0.99±0.005	1.01±0.006	0	1	2-2.6
PS 0.5K	$0.52±3\cdot10^{-4}$	$0.59±2\cdot10^{-4}$	$1.38±5\cdot10^{-5}$	$1.35±3\ 10^{-5}$	13.5	1	0.2-1.8
	0.50±0.004	0.56±0.003	$1.38±8\cdot10^{-4}$	$1.35±6\cdot10^{-4}$	12	2	0.2-1.8
Glycerol	0.048±0.015	0.53±0.01	1.56±0.004	1.54±0.004	10.4	1	1.4-1.6
PC	0.27±0.0017	0.36±0.003	$1.42±4\cdot10^{-4}$	$1.41±6\cdot10^{-4}$	32.4	2	0.33-1.45
	0.39±0.001	0.53±0.003	$1.42±3\cdot10^{-4}$	$1.41±9\cdot10^{-4}$	35.9	1	1.26-1.45
PG	0.33±0.004	0.36±0.003	$1.47±4\cdot10^{-4}$	$1.44±3\cdot10^{-4}$	9	1	1.3-1.55
SB	0.62±0.002	0.74±0.001	$1.34±4\cdot10^{-4}$	$1.32±3\cdot10^{-4}$	19.3	2	0.4-1.44
	0.76±0.002	0.91±0.005	$1.34±3\cdot10^{-4}$	$1.32±3\cdot10^{-4}$	19.7	1	1.06-1.44